

## Residual stresses and imperfections in welded high-strength I-shape sections

H. Pasternak & B. Launert

*Chair of Steel and Timber Structures, Brandenburg University of Technology (BTU), Cottbus, Germany*

T. Kannengießer & M. Rhode

*Department 9.4—Weld Mechanics, BAM Federal Institute of Materials Research and Testing, Berlin, Germany*

**ABSTRACT:** This article addresses the imperfections caused by the weld assembly in I-shape sections made of two structural steel grades. Load influencing imperfections are assumed as deviations from the ideal shape (e.g. bending distortion) and longitudinal residual stresses. The quality of a numerically aided design of components exposed to either compression and/or bending is significantly affected, depending on these parameters [1]. The Eurocode provides robust simplified models. As a result, the Ultimate Limit State (ULS) is approached on a conservative basis. The following investigations are aimed at providing further guidance on these values in component-like specimens. The long term goal is an improved understanding of the load-bearing capacity of such sections. As a first step in this process, the experimental and corresponding numerical studies are presented

### 1 INTRODUCTION

The implementation of imperfections is a major task in the performance of any nonlinear FE-simulation. An appropriate method to describe the behavior at Ultimate Limit State (ULS) is a calculation where the material and the geometry behavior are nonlinear. The imperfections guide or support the subsequent failure. Therefore, the implemented imperfection pattern has usually a strong influence on the ultimate load.

With modern FE codes it is possible to include geometrical (e.g. global bow imperfections) and structural imperfections (mainly residual stresses) separately. This is also the best way to access their influence correct. The general influence of residual stresses is to cause premature yielding. The typical yield zone patterns at ULS are given exemplary for pure compression and 3-point bending in Fig. 1. Both cases show more or less similar yielding over wide areas of the corresponding side of the chords in compression.

From Fig. 1 can be concluded that the dominating factor with respect to residual stresses is the values along the edge of the chords. Their influence is at its maximum for a relative slenderness which is close to 1 or below depending on the type of failure. For the flexural buckling failure, investigations in [1] have shown the influence to be the bigger, the lower the relative slenderness (up to

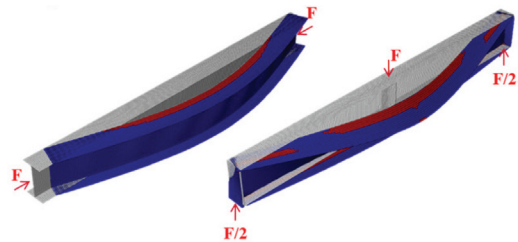


Figure 1. Yielding at ULS for pure compression and 3-point bending.

some lower limit where the cross-section resistance determines the ultimate load).

The assignment to a buckling curve (according to Eurocode) is typically one or two curves below the corresponding curve for sections manufactured by hot rolling. Especially for grades higher than S460, the assignment is conservative because the same classification is applied irrespectively of the grade. This is limiting the application of high-strength steel for welded profiles. However, recent studies have shown that the assumption of tensile stresses equal to the yield stress tends to overestimate the residual stresses [2]. Nevertheless, no firm conclusion has been drawn yet.

For that, a national research work is carried out to develop advanced models for the implementation of weld-induced imperfections. The following

sections present the experimental as well as corresponding numerical studies:

The experiments are divided into three parts: (1) a study on the influence of the edge preparation by flame cutting of the chord edges, (2) residual stress measurements on I-girders by sectioning method and (3) measurements of the initial geometry on full-size samples.

The FE-simulations contain models for the global (or also called structural) welding simulation of a representative structure part. The length is reduced to a necessary minimum to create uniform residual stresses at mid length. The models are subsequently used to decide on some advanced residual stress models.

## 2 INFLUENCE OF EDGE PREPARATION ON RESIDUAL STRESSES

### 2.1 Edge preparation by flame cutting

It is known that the cutting method has an influence on the residual stresses [3]. In steel construction, the cutting is typically realized by flame cuts. The metal is heated by a torch to its kindling temperature and is oxidized by a stream of oxygen from the torch. The process involves intense local heating and rapid cooling along the cutting edge. Consequently, the formation of residual stresses is quite comparable with the processes caused by welding. Thus, tensile residual stresses near the cutting edge superpose with welding residual stresses leading to a reduction or reversal of compressive residual stresses along the cutting edge. A numerical study taking into account this effect has shown beneficial effects on the load-carrying capacity in compression due to the delay in yielding [4].

### 2.2 Results

The results of a preliminary study to systemize such effects are presented. In a first step the base plate is cut and measured by X-Ray Diffraction (XRD). Secondly, a stiffener is welded in the chord center line with two fillet welds by MAG process. After that the XRD measurement is repeated. The width of the chord is 150 mm. The results are shown in Fig. 2.

The saw cut induces no remarkable residual stresses. After welding of the stiffener, the stresses are shifted by a more or less constant value to a maximum of 200 MPa in compression. In contrast, flame cutting induces tensile residual stresses near the yield stress. As a result, the stresses along this edge remain in tension or close to 0 after welding. The affected area is limited to about 15 mm. In [3] this value is given by the chord thickness (which is 20 mm in here).

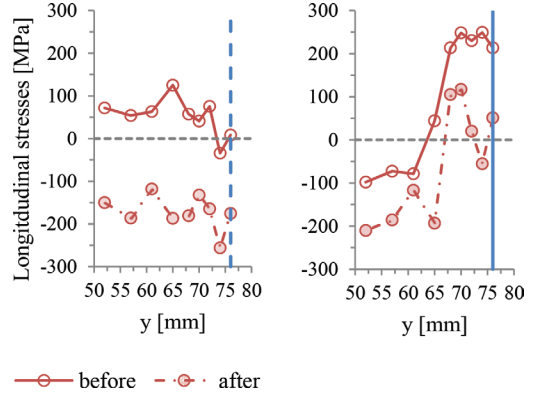


Figure 2. Influence of the edge preparation (saw cut: dashed vertical line, flame cut: solid vertical line) on the residual stresses before and after welding (chord is 20 mm, stiffener is 10 mm, material is S355J2+N and energy per unit length is at  $9,2 \cdot 10^{-3}$  J/mm).

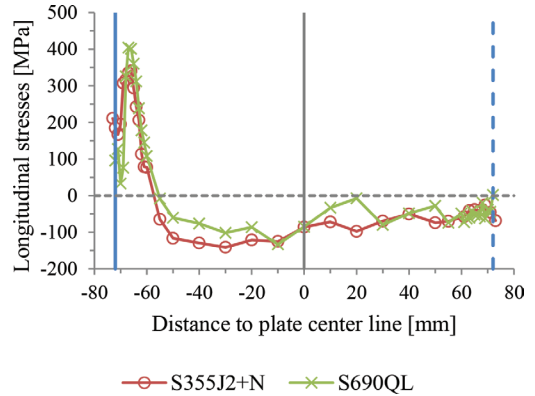


Figure 3. Influence of the edge preparation (saw cut: dashed vertical line, flame cut: solid vertical line) on the residual stresses before welding (chord is 25 mm, materials are S355J2+N and S690QL).

A further comparison of residual stresses after cutting for S355 and S690 is given in Fig. 3. To limit the number of specimens, one edge is saw cut, the other is flame cut. The stresses are at a similar level for both materials. Tensile residual stresses reach a maximum of about 350 MPa for S355 and 400 MPa for S690.

## 3 RESIDUAL STRESS MEASUREMENTS

### 3.1 Program

To investigate the welding effect on the residual stresses, eight I-girders were manufactured by MAG process. The base materials are S355J2+N

and S690QL. The filler materials are commercially available G4Si1 for S355 and Mn4Ni1, 5CrMo for S690. The chords are 150 mm and the web is 220 mm in all specimens. The edge preparation was realized by waterjet-cutting to reduce initial stresses prior to welding. The plate thicknesses are either 25 mm or 15 mm in the chords and 15 mm or 10 mm in the web. The weld type is a one-layer fillet weld, and all welds were deposited subsequently after each other. The setup is given in Fig. 4. Each weld seam is approximately 1 m to ensure uniform residual stresses. The parameters are given exemplary for girders with 25 mm in the chords and 15 mm in the web in Table 1.

### 3.2 Sectioning method

The residual stresses have been measured at BAM Federal Institute of Materials Research and Testing using the sectioning method. The measurement by sectioning method has proven to be adequate for the determination of (mainly longitudinal) residual stresses in large structural components in the past [5]. For that, the girders are vertically sectioned by saw cutting. Each sectioning causes the release of residual stresses by relaxation processes. The elastic relaxation strains are measured by strain gauges in longitudinal (and transverse) direction. The residual stresses can be calculated by Eq. 1. This method can be further simplified if transverse strain is assumed to be negligible.



Figure 4. Test setup for the manufacture of welded I-girders, MAG welding tractor.

Table 1. Parameters for girders with chords 25 mm and web 15 mm.

Grade	S355J2+N		S690QL	
	S1	S2	W1	W2
No.				
I [A]	338	327	324	329
U [V]	33,4	33,4	33,7	33,7
v [mm/s]	8,17	5,17	8,17	5,17
$\bar{Q}$ [J/mm]	$1,39 \cdot 10^{-3}$	$2,11 \cdot 10^{-3}$	$1,34 \cdot 10^{-3}$	$2,14 \cdot 10^{-3}$

$$\sigma = -\frac{E}{1-\nu^2} \cdot (\varepsilon_1 + \nu \cdot \varepsilon_2) \quad (1)$$

where,  $\sigma$  is the calculated longitudinal stress in MPa,  $\varepsilon$  is the measured relaxed elastic strain.  $E$  is the Young's modulus in MPa and  $\nu$  is the Poisson's ratio. Index 1 indicates the longitudinal direction in the direction of the weld seam. Index 2 indicates the transverse direction.

In total, 24 strain gauges (at 12 measuring positions) were applied for one quarter of the section assuming a more or less symmetrical distribution of residual stresses. The strain gauges were applied on the inner and outer side of the chords and the web. In the next step, XRD will be used on the remaining sections to determine those stresses which were not relaxed due to sectioning.

### 3.3 Results

The results by sectioning are referred to the mean values of yield stress (based on minimum 5 tensile tests per plate). Values for the chords are given in Fig. 5.

It is noticed that normalized stresses for S690 are at approximately half of the corresponding values for S355. The importance of longitudinal residual stresses is therefore reduced. No conclusion can be drawn for the tensile stresses yet. Nevertheless, the increase in tension seems less steep. Apart from that, it is demonstrated how the increase in the weld heat input (indicated by the index 1 or 2) acts on the magnitudes in compression. An increase of

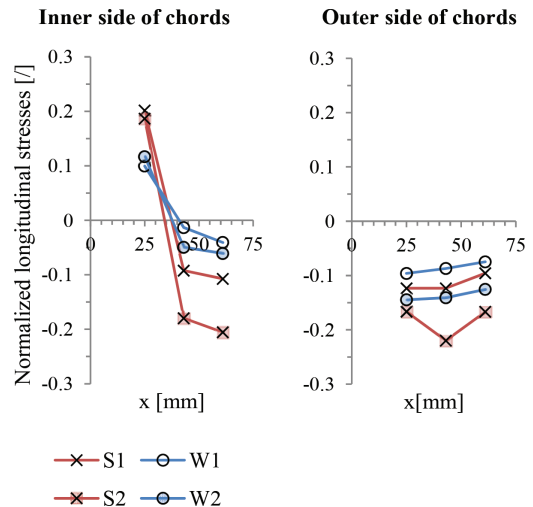


Figure 5. Normalized longitudinal residual stresses for the chord (referred to  $R_{p0.2} = 463,9$  MPa for S355 and 840,8 MPa for S690).

weld heat input with otherwise the same conditions seems to influence less on S690 compared to S355 (due to the increased yield stress). The gradients through the thickness at the same energy input are also stronger for S690.

## 4 NUMERICAL SIMULATION

### 4.1 Numerical model for welding

The experimental results are typically limited in accessibility (it is not possible to take a look inside the component) and number of points. A simulation aims to increase the density of information and helps to create a complete understanding of the process. Welding simulation in the structural context means that the macro behavior under local heat input is simulated. For that, heat is introduced either by the definition of temperatures or temperature isotherms (in °C) or by an idealized heat source model which estimates the distribution of heat (in  $W/mm^3$ ). Also, the temperature field and the mechanics are usually determined in separate runs (as the coupling applies mainly in one direction). If the microstructure is of importance, an additional step is inserted. For that, several empirical and semi-empirical models are available [1].

The specific calculation in this study was carried out using specialized software (Simufact, V. 5.0.0). It provides the advantage of standardized necessary input data (such as material library, heat source models, weld path definitions, solver settings etc.). On the other hand, this may also restrict the user in some applications. The implemented model is shown in Fig. 6.

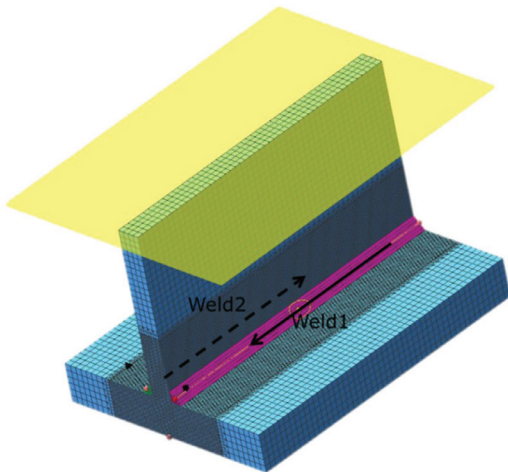


Figure 6. Numerical model of half girder with symmetry about the web.

The model was build using symmetry about the web (assuming that due to the web height opposite welds do not affect one another). The length of the model is 200 mm. No gap is modelled (the parts are assumed to be one solid piece). The consideration of a gap (contact problem) increases the calculation times and might be linked to numerical problems. However, especially for the stresses this effect is negligible.

The element edge length close to the weld (40 mm) is approximately 1 mm. Far from the weld, elements are 5 mm. The element types are assigned automatically by the software. For thermal analysis 8-node heat transfer bricks are used (MSC.MARC, element 43), and 8-node isoparametric bricks are used for mechanics (element 7). The total number of elements in this model is 565.000. The sequencing was simplified. Pause times between welds were not taken into account, because temperatures are already dropped at the end of each weld (due to the plate thickness). The time stepping is set adaptive (i.e. variable time steps). And the end time is 250 s in all models.

The materials are taken from the library as S355J2G3 and S690QL. In a first approach, Single Phase Models (SPM) are used. In terms of global compressive residual stresses this is sufficient as a first approximation. Comparative calculations for S355 have shown that the implementation of Multi Phase Models (MPM) does not influence the result significantly [1]. The stress-strain behaviour was scaled. This is recommended in general, because the yield stress is linked with the exteriors of the plastic zone, and consequently also with the compressive residual stresses.

### 4.2 Results

In the following, results are given for S1 and W1. The calculated (longitudinal) residual stresses are given in comparison to the measured values in Fig. 7 and 8.

It should be considered that the measured residual stresses by sectioning method represent “global” stresses released over a certain volume. In contrast, values at the exteriors of the model are plotted for the numerical model. The agreement is therefore evaluated on average. A good correlation with the compressive residual stresses is noticed. However, the numerically calculated residual stresses close to the weld seam are currently questionable (inner side of the chords especially for S690). The effect of phase transformations needs to be added (recently in progress).

The compressive residual stresses seem to be more or less at a similar level (irrespectively of the grade). With respect to the yield stress, the influence of longitudinal residual welding stresses is hence significantly reduced for S690 (the same was noticed in Fig. 5).

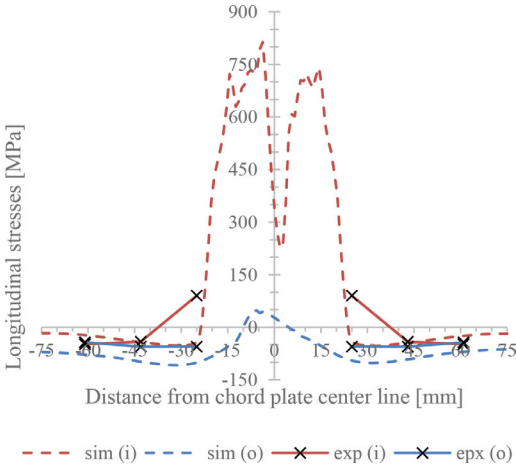


Figure 7. Longitudinal residual stresses on the inner (i) and outer side (o) of the chords, S355.

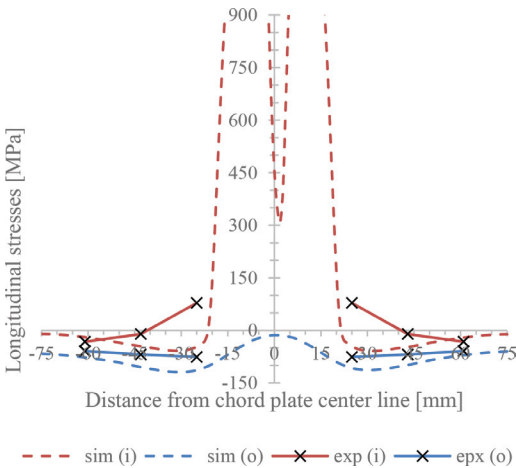


Figure 8. Longitudinal residual stresses on the inner (i) and outer side (o) of the chords, S690.

It should be highlighted that the computation times even though to various simplifications range at a few days, in here between 5 to 6 days using DDM (Domain Decomposition Method) with 4 domains in longitudinal direction. Computer was a standard working station (2x Intel Xeon E5-2670, 64 GB RAM). Thus, a simplified modelling procedure is needed. In the following, reference is made to the numerical models.

## 5 RESIDUAL STRESS MODELS

### 5.1 Review of existing theories

A summary of some simplified models can be found e.g. in [6]. However, none of the models

are considered adequate. A quite general problem what applies to all available simplified models is that no validity range is given. Hence, the agreement may range from sufficient to inappropriate within the same model. An advanced empirical model needs to account for the plate thickness and the heat input with reference to different structural steel grades (it has been shown e.g. that reduced normalized values apply for S690). The edge preparation is to be taken into account too.

### 5.2 Advanced models

The weld influence can be captured fast and with usually sufficient agreement using mechanically equivalent models. The principle of such approach is to reduce the complex thermo-mechanical problem to the mechanical level. Initially, it is important to understand the cause of the remaining residual stresses.

This is illustrated considering a clamped bar fixed at both ends which is exposed to different maximum temperatures (bar theory). In the simplest form, the strains are composed of elastic strains  $\epsilon^e$ , plastic strains  $\epsilon^p$  and thermal strains  $\epsilon^{th}$ . The model is shown in Fig. 9.

As long as the thermal strain  $\epsilon^{th}$  is below the strain to cause yielding, no stresses remain after cooling to room temperature. Consequently, the plastic strain (also incompatible or inherent strain) causes residual stresses [7]. The degree of restraint against thermal expansion is usually close to a fixed condition.

The plastic strains can be computed numerically using either two-dimensional (2-D) or three-dimensional (3-D) thermo-elasto-plastic analysis on finite element models of simple weld geometry. Subsequently those are mapped to the full structure finite element model and a linear-elastic analysis is carried out. This principle has been used in different ways by different authors, mainly

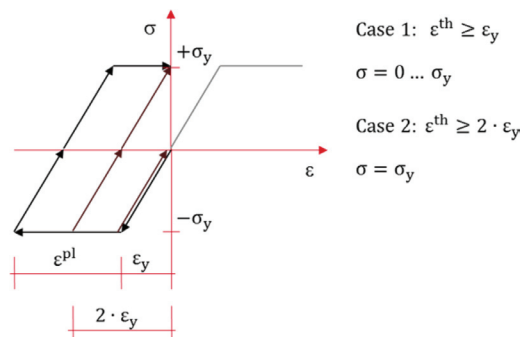


Figure 9. Stress-Strain ( $\epsilon^e + \epsilon^p$ ) correlation due to bar theory (ideal elasto-plastic material behavior).



in the mechanical engineering sector (also known as Inherent Strain Method or with reference to an equivalent force also as Equivalent Load Method or Shrinkage Force Method).

A promising approach in this context is especially the combined analytical-numerical hybrid shrinkage model by [8]. However, no record was taken of the residual stresses yet. The numerical calculation of plastic strains is replaced by an advanced (iterative) analytical model which is used to calculate the shrinkage forces (or more generally the shrinkage volume) in longitudinal and transverse direction and their corresponding load application points. The shrinkage force may be compared to a tendon which is first prestressed and then applied eccentrically to the structure. Such force is typically high and will lead to very local deformations which may cause numerical problems. At the same time compressive residual stresses are introduced in the weld seam close area. This is why strains are used instead. The shrinkage force is the volume integral of these strains. The strains are linearly distributed through the thickness.

An example of this method for the girder S1 is shown in Fig. 10. The residual stresses close to the weld and in the adjacent parts of the structure are given with the correct signs. The magnitudes in compression seem to be valid in comparison to the results given in 4. The implemented data are the width of the plastic zone, the size of plastic strains and the corresponding application points needed to distribute the strains (linearly) through the thickness. To calculate the longitudinal stresses (and bending deformations), the model can be further simplified by assuming the transverse strain to be negligible. This assumption applies to girders with the dominant direction in longitudinal direc-

tion. The computation time for this example is somewhere at a minute or less. Thus, such approach is practically of particular interest (especially for application to large structural components).

The values needed for implementation of the model were calculated based on a T-joint with one fillet. Subsequently the same values were applied to all welds. This requires a symmetric distribution of residual stresses (which seems sufficient as a first approach). If the initial stresses (due to the first weld) are taken into account for the second weld and so on, this would result in a non-symmetric stress state (and a remaining bending distortion). With the previous assumptions, no bending occurs due to symmetry.

For a fast approximation of the dimensions of the plastic zone, the maximum temperature isotherms may be used. A thermal analysis is usually fast and thermo-physical properties are widely known (and are quite constant for all low-alloyed structural steel grades). The corresponding temperatures (to cause longitudinal plastic strain) can be given based on bar theory (Fig. 9).

$$\Delta T_2 = \frac{2 \cdot \varepsilon_y}{\alpha} = \frac{2 \cdot \sigma_y}{\alpha \cdot E} \quad (2)$$

$$\Delta T_1 = \frac{\sigma_y}{\alpha \cdot E} \quad (3)$$

where,  $\Delta T$  is the temperature difference in K,  $\varepsilon_y$  is the yield strain,  $\sigma_y$  is the yield stress in MPa,  $E$  is the Young's modulus in MPa and  $\alpha$  is the thermal expansion coefficient in 1/K.

From Eq. 2 and 3 is concluded that the temperature difference to cause plastic strains is the bigger, the higher the yield stress and the lower the Young's modulus and the thermal expansion coefficient. Consequently, the plastic zone is reduced for higher structural steel grades. E.g. for S690 the relevant temperatures are almost twice as high as for S355. This is related to a stronger gradient through the thickness and on average reduced tensile residual stresses, and consequently also reduced compressive residual stresses (both with respect to the yield stress).

## 6 INITIAL DEFORMATIONS

### 6.1 Tolerances

The geometric deviations are typically assumed in common with the tolerance limits prescribed in EN 1090-2 and a suggested reduction to 80% of this value in EN 1993-1-5 (due to a probabilistic safety concept). Assuming that the statistical distribution of the initial deformations was a known input, it would be possible to calculate the design value to

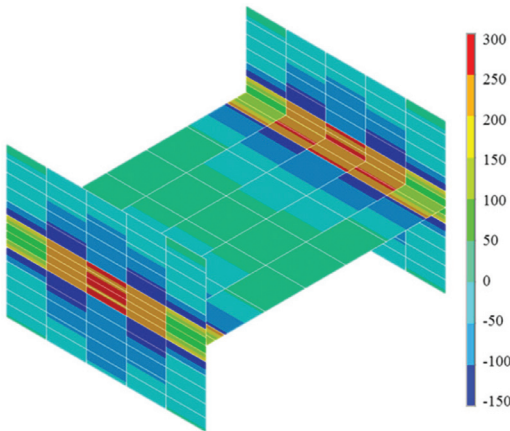


Figure 10. Calculated (longitudinal) residual stresses (in MPa), hybrid shrinkage model, Ansys, V. 14-5.

be used [9]. However, systematic measurements are rarely available.

For the section types investigated in this study (only class 1 and 2), the ULS is influenced by bow imperfections in each y- and z-direction. The initial out-of-straightness is limited to  $L/750$  (irrespectively of the direction). The more established value of  $L/1000$  is equal to approximately 80% of this value (see above).

The value of  $L/1000$  was used by the European Convention for Constructional Steelwork (ECCS) during the development of European column curves. The initial out-of-straightness is basically a function of the manufacturing process, and some column types tend to be very straight. Nevertheless, in the development of multiple column curves the position was taken that the initial amplitude of  $L/1000$  seems to be a reasonable value. The US Structural Stability Research Council (SSRC) took a different position and recommended using  $L/1500$  instead, because this was closer to the average ( $L/1470$ ) measured in laboratory columns. This value was also adopted by AISC as the governing out-of-straightness criterion [10].

The implemented shape is usually sinusoidal. The real configuration may be complicated though and does not necessarily have its maximum in the center. Therefore, modified amplitudes (for the model with sinusoidal shape) were recalculated from available measurements. Those values vary between  $L/530$  and  $L/3360$  [11].

The effect of an additional eccentricity was not taken into account. This is on purpose, because there are really no truly pin-ended columns in existence. Therefore, the technically unavoidable presence of such eccentricity is of less importance compared to the correct assessment of the buckling length. At the same time, this value is difficult to measure, because it is related to the assembly on site and usually not accessible.

## 6.2 Measurements

Reliable data for welded sections are generally quite limited. Data by Chernenko and Kennedy [12] indicate a relatively small initial crookedness with an average of approximately  $L/3300$ . Having this in mind, one should generally expect smaller values than those prescribed by the standard. For a further categorization, extensive 3D-measurements on six girders of a length of 2500 mm were carried out. The plate thickness is 20 mm in the chords and 10 mm in the web. Grade is S355J2+N. Welding processes are MAG and SAW with three equally welded girders for each process.

It should be considered carefully that the values of interest range at a few mm (or less). Hence, those are very difficult to measure with conven-

tional methods. All specimens were completely digitalized using a photogrammetry system (TRITOP) together with a 3D-scanner (ATOS II Triple Scan) by GOM. The accuracy is at approximately 0,03–0,04 mm. Based on the digital 3-D model, sections at a certain interval were created, from where the center of each section was determined. This allows for an “exact” statement on the initial out-of-straightness (defined as deviations to a straight line connecting the end center points).

The evaluation is recently being processed. The results are of complex shape for all specimens. It was already noticed that the deformations are quite different with regard to the axis. This is probably due to the sequencing of welds. Values tend to be generally higher for the deformation about the strong girder axis. A numerical study may help as well to understand the influence of different parameters. Such study is only possible using one of the models proposed in 5.

## 7 CONCLUSIONS

The article has given an overview on residual stresses and deformations present in welded I-shape sections. The results have led to the following main conclusions:

- The edge preparation by flame cutting induces remarkable longitudinal tensile residual stresses. Values were at the same level for S355 and S690. Those stresses superpose with the stresses caused by welding.
- The residual stress measurements by sectioning method have shown to be adequate to determine longitudinal residual stresses in large structural components. The S690 has shown significantly reduced normalized longitudinal residual stresses underlining their decreased importance in high strength steel.
- The numerical welding simulation has shown a sufficient agreement with experimental data. The tensile residual stresses close to the weld require further investigations. Nevertheless, the global distribution seems to be more or less independent of that.
- The effort to run such simulation is still not in a practically applicable range. For that purpose, simplified models are still in need. However, none of the available (empirical) models seems sufficient.
- The residual stresses (and also deformations) can be calculated much better using mechanically equivalent models (plasticity based approach). A proposal how such procedure is implemented was described. Verification with thermo-elasto-plastic models is needed.

- The initial out-of-straightness has to be further categorized. A uniform definition irrespectively of the cross-section type and the manufacturing method is necessarily conservative. A basis study was started, but in general more measurements are required.

## ACKNOWLEDGEMENTS

The authors thank the German Federation of Industrial Research Associations (AiF) for the financial support of the research project IGF-No. 18104 BG. This project is carried out under the auspices of AiF and funded by the Federal Ministry for Economic Affairs and Energy (BMWi) as part of the programme to support Industrial Community Research and Development (IGF).

## REFERENCES

- [1] Pasternak, H., Launert, B., Krausche, T.: Welding of girders with thick plates—Fabrication, measurement and simulation, *Journal of Constructional Steel Research*, 115, 407–416, 2015.
- [2] Clarin, M.: High Strength Steel: *Local Buckling and Residual Stresses* (PhD-Thesis), Lulea University of Technology, Sweden, 2004.
- [3] Beg, D., Hladnik, L.: Residual Stresses in welded I-profiles made of high strength steel (in German), *Stahlbau*, 63(5), 134–139, 1994.
- [4] Pasternak, H., Launert, B.: Improved design approaches for the load bearing capacity of welded I-profiles from high strength steel considering realistic residual stresses, *7th European Conference on Steel and Composite Structures*, Naples, Italy, 159–160, 2014.
- [5] Rossini, N.S., Dassisti, M., Benyounis, K.Y., Olabi, A.G.: Methods of measuring residual stresses in components, *Materials and Design*, 35, 572–588, 2012.
- [6] Chacon, R., Serrat, M., Real, E.: The influence of structural imperfections on the resistance of plate girders to patch loading, *Thin-Walled Structures*, 53, 15–25, 2012.
- [7] Ueda, Y., Yuan, M.G.: The Characteristics of the Source of Welding Residual Stress (Inherent Strain) and its Application to Measurement and Prediction, *Trans. of JWRI*, 20(2), 119–127, 1991.
- [8] Michailov, V., Stapelfeld, C., Doynov, N.: *Upgrade of an analytical hybrid model for the distortion simulation of large structures* (in German), Forschung für die Praxis P 868, Düsseldorf, 2014.
- [9] Johansson, B., Maquoi, R., Sedlacek, G., Müller, C., Beg, D.: *Commentary and Worked Examples to EN 1993-1-5: Plated Structural Elements* (JRC Scientific and Technical Reports), Luxembourg: Office for Official Publications of the European Communities, Luxembourg, 2007.
- [10] Ziemian, R.D. (editor): *Guide to Stability Design Criteria for Metal Structures*, Sixth Edition, John Wiley & Sons, 2010.
- [11] ECCS European Convention for Constructional Steelwork (Committee 8): *Manual on Stability of Steel Structures*, Second Edition, 1976.
- [12] Chernenko, D.E., Kennedy, D.J.L.: An Analysis of the Performance of Welded Wide Flange Columns, *Canadian Journal of Civil Engineering*, 18, 537–555, 1991.